Techno-economic analysis of expander-based configurations for natural gas liquefaction

Nagy, Matteo ; Nguyen, Tuong-Van; Elmegaard, Brian; Lazzaretto, Andrea

Published in:
Proceedings of ECOS 2017: 30th International Conference on Efficiency, Cost, Optimization, Simulation and Environmental Impact of Energy Systems

Publication date:
2017

Document Version
Peer reviewed version

Techno-economic analysis of expander-based configurations for natural gas liquefaction

Matteo Nagy[a], Tuong-Van Nguyen[b], Brian Elmegaard[c] and Andrea Lazzaretto[d]

[a] Burmeister & Wain Scandinavian Contractors A/S, Allerød, Denmark, matn@bwsc.dk
[b] Technical University of Denmark, Kgs. Lyngby, Denmark, tungu@mek.dtu.dk,
[c] Technical University of Denmark, Kgs. Lyngby, Denmark, be@mek.dtu.dk
[d] Università degli Studi di Padova, Padova, Italy, andrea.lazzaretto@unipd.it

Abstract:
The use of liquefied natural gas (LNG) as a marine fuel is rapidly growing because of the possible economic advantages over conventional fuels and stricter environmental regulations. Production of LNG is energy-intensive because of the required temperature level of around -160°C. Three main types of refrigeration cycles have been developed. The present work focuses on the comparison of six expander-based configurations, which in spite of the higher power consumption are more compact, flexible and easier to operate. They are optimised from a thermodynamic perspective: the exergetic efficiency ranges between 15.5 % and 30 % for a specific power consumption from 2570 kJ/kg down to 1340 kJ/kg.
Multi-objective optimisations are performed to simultaneously minimise the net power consumption and the heat transfer conductance as an indicator of the required heat transfer area. The latter ranges between 50 kW/K and 275 kW/K.
A trade-off between the power consumption and heat transfer area is found, which justifies a further economic analysis. A simplified economic analysis is set based on a discounted cash flow model. The unitary profit ranges between 0.3 and 0.85 DKK per kg of produced LNG. The most profitable expander-based configuration is the dual-refrigerant cycle with nitrogen in the bottoming cycle. Finally, the influence of the cost correlations on the economic outcome is assessed: the compressors represent the major costs, which leads to the coincidence of the thermodynamic and economic optima.

Keywords: natural gas liquefaction, expander-based cycles, process modelling, thermodynamic optimization, exergy analysis, economic analysis.

1. Introduction

Liquefied natural gas (LNG) is a liquid mixture of hydrocarbons consisting mainly of methane, with small fractions of ethane and propane. It is produced at around -160°C, and stored at low to near atmospheric pressures. The higher heating value of LNG ranges between 45 and 50 MJ/kg, which is greater than typical hydrocarbon-based fuels such as diesel. The energy density of LNG ranges between 20 MJ/litre and 22 MJ/litre (HHV basis), which is about 2.5 times greater than compressed natural gas (CNG), making it interesting for transportation and storage purposes [1]. In addition, LNG is a cleaner fuel than conventional fossil fuels such as diesel oil because of the lower emissions of sulphur (SO_x) and nitrous (NO_x) oxides in the combustion process.
The interest for LNG has therefore grown in several sectors, such as the shipping and petrochemical industries. The former sector faces more severe environmental regulations in areas such as the coastal areas of Canada and United States, the Baltic Sea and the North Sea [2], [3]. Substituting heavy fuel oils for natural gas is therefore a promising option from both environmental and economic perspectives. The latter sector faces high volatility of the oil and gas price and the current petroleum resources are getting depleted. Valorising and liquefying the produced gas from conventional and unconventional oil fields is thus a possibility under study.
The production of LNG has grown exponentially in the last decades. At present, the installed capacity exceeds 320 mtpa (million tonnes per annum) worldwide. Around 6 % correspond to small-scale plants, i.e. with a production capacity smaller than 1 mtpa per unit [4]. Liquefaction systems generally include a pre-treatment process upstream, where carbon dioxide, hydrogen sulphide and water are removed to avoid corrosion and plugging issues at cryogenic temperatures. They are based on refrigeration cycles that can be grouped in three categories: the cascade, the mixed-refrigerant and

the expander-based processes. They present different process layouts, working fluids, operating conditions and machinery.

In a cascade system, natural gas is liquefied in three main steps – pre-cooling, liquefaction and sub-cooling. A dedicated refrigeration cycle is used for each step, using pure fluids such as propane, ethylene or ethane, and methane [5]. Cascade systems are currently the most energy-efficient processes and are considered as a reference for large-scale LNG production. Expander-based systems present a lower performance, because of the large gaps between the temperature-enthalpy profiles of the natural gas and refrigerant. However, these systems require fewer components than a conventional cascade system (lower equipment inventory), since fewer heat exchangers are needed. As a difference from cascade and mixed-refrigerant processes, the refrigerant is always in gaseous form, and only the sensible heat is used in the refrigeration process. This avoids maldistribution issues of the two-phase fluid in the cryogenic heat exchangers, which is an interesting advantage for systems in motion [6]. Moreover, the refrigerant preferably used in expander-based processes is generally a pure fluid, either nitrogen or methane. Hence the refrigeration process is easier to operate and control, as there is no need to adjust the fluid composition if the feed properties vary with time. These advantages are of particular relevance for LNG applications such as small-scale or offshore systems, where operational simplicity, safety, weight and footprint are important factors. Expander-based processes seem competitive for these applications, and much research was conducted in the last decade to investigate how their performance can be improved. Finn [7] compares them against mixed-refrigerant systems for small-scale applications, and concludes that both types of cycles can be competitive for such sizes. Cao et al. [8] assess the performance of two types of LNG processes in skid-mounted packages. They state that a nitrogen-methane cycle can present a higher performance than single mixed-refrigerant processes if there is no propane pre-cooling (PRICO). Remeljej and Hoadley [9] evaluate the efficiency of four small-scale liquefaction systems, of which three are expander-based processes. They conclude that the mixed-refrigerant process is the least energy-intensive, and that the performance of open-loop expansion processes is very sensitive to variations of the feed gas composition. Shah and Hoadley [10] develop an optimisation method based on the minimisation of the shaft work demand in expander cycles. Castillo and Dorao [11] perform detailed cost analyses for expander-based and mixed-refrigerant processes and propose decision-making methods. He and Ju [12] simulate sixteen layouts of expander-based systems for distributed scale and optimise them, maximising their second law efficiency. They suggest the addition of a pre-cooling cycle to improve the system performance by more than 20 %. Such solutions result in a more complex setup, without compromising the other advantages of expander-based processes (non-sensitivity to motion, gaseous refrigerant, etc.). Chang et al. [13] assess the maximum performance that can be reached, in theory, with expander-based processes. This work demonstrates that such systems can compete and even be superior to mixed-refrigerant processes.

Limited research on comparing and optimising several layouts of expander-based processes from both a thermodynamic and economic perspective has been presented. Therefore the present work aims to address these gaps and focuses on the modelling and optimisation of expander-based processes. It builds on the analysis of six configurations (single, dual-expansion and dual-refrigerant cycles) that have been described in the scientific literature. The aim is twofold. First, the authors assess the thermodynamic performance of each process and analyse relevant improvements based on optimisation routines. Secondly, an economic evaluation is performed to depict the most profitable configuration.

2. Process description

The expander-based concept builds on different layouts of the reverse Brayton cycle, where the working fluid is compressed and expanded through a turbine to generate the refrigeration effect. The refrigerant is nitrogen or methane and stays always in the gaseous form, allowing for plant safety, simplicity and ease of operation compared to refrigeration cycles operating with hydrocarbon and nitrogen mixtures undergoing phase change.

Six different expander-based configurations are investigated and here introduced. The respective process flow sheets are depicted in Figures from 1 to 6.
In the simplest configuration (Figure 1), nitrogen is compressed (process 11-12) and after-cooled (process 12-7) before entering the cold box. The refrigeration requirement for natural gas liquefaction and sub-cooling is provided through a work-producing expansion (process 8-9). Nitrogen at the turbine outlet is in super-heated or saturated conditions. The compression process can be designed into one (Figure 1) or two inter-cooled stages (Figure 2).
A first development is given by the addition of a pre-cooling stage to the single-expander configuration using propane as refrigeration medium (Figure 3). The pre-cooling cycle is a single-stage sub-critical refrigeration cycle, providing pre-cooling for both natural gas feed and nitrogen in the main refrigeration cycle.
Additionally, the expansion process can be performed in two stages (Figure 4), with only a fraction of the refrigerant nitrogen undergoing the low-pressure expansion (process 13-14). A dual-expansion process entails a two-stage compression process, such that the intermediate-pressure and low-pressure nitrogen streams mix without major energy loss.

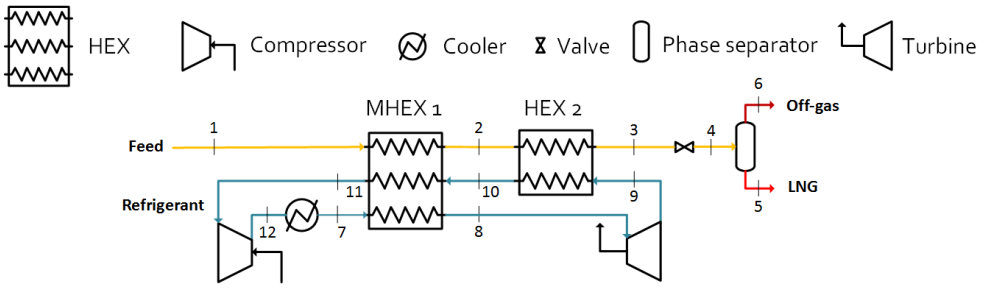

Figure 1: Single-expander configuration with one compression stage

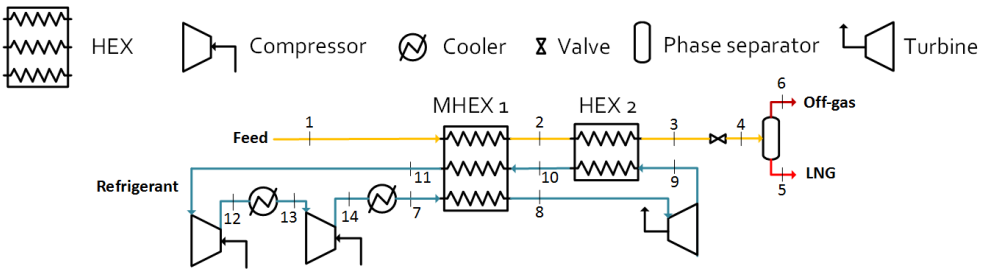

Figure 2: Single-expander configuration with two compression stages

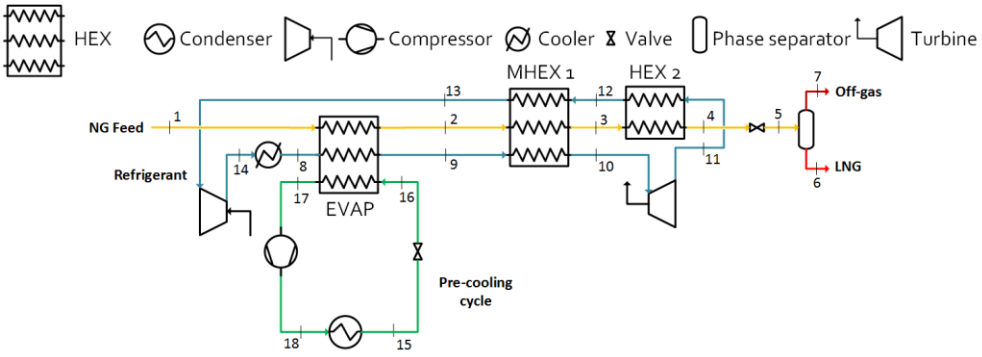

Figure 3: Propane pre-cooled single-expander configuration

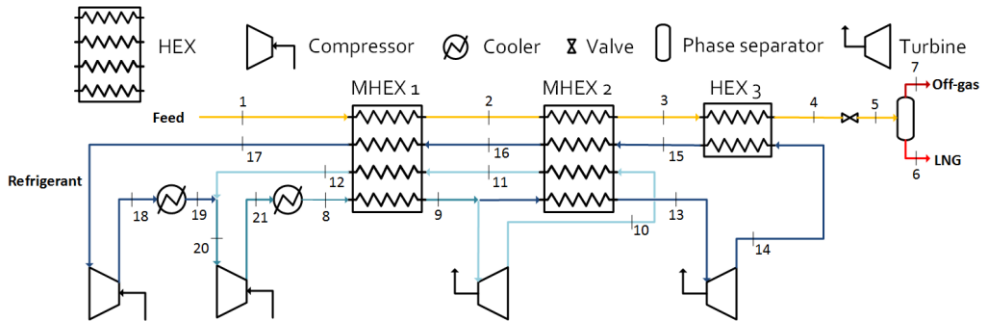

Figure 4: Dual-expander configuration

Finally a dual-refrigerant configuration is obtained coupling in series two single-expander configurations, with one cycle using nitrogen and the other employing methane. Both possibilities are included in the present work (Figure 5 and Figure 6).

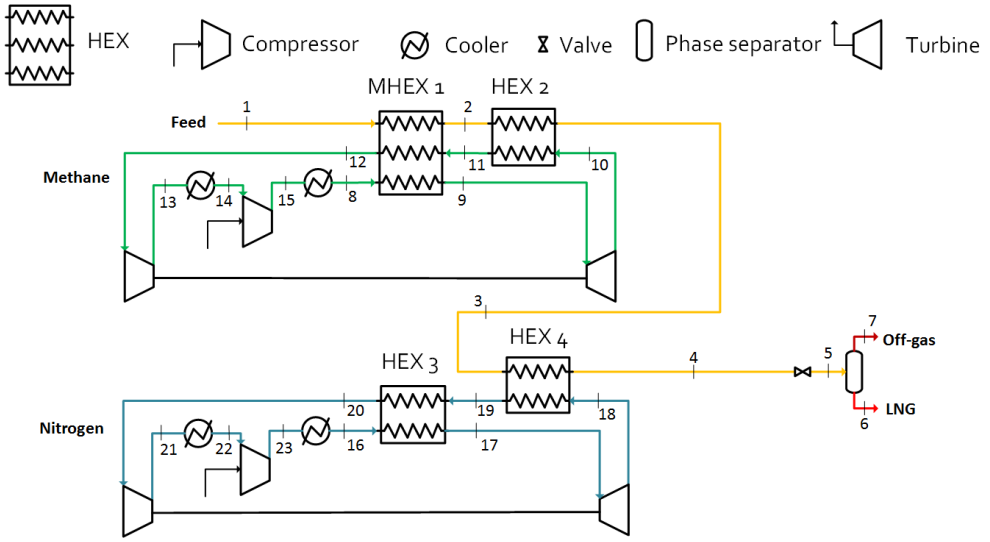

Figure 5: Dual-refrigerant configuration with nitrogen in the bottoming cycle

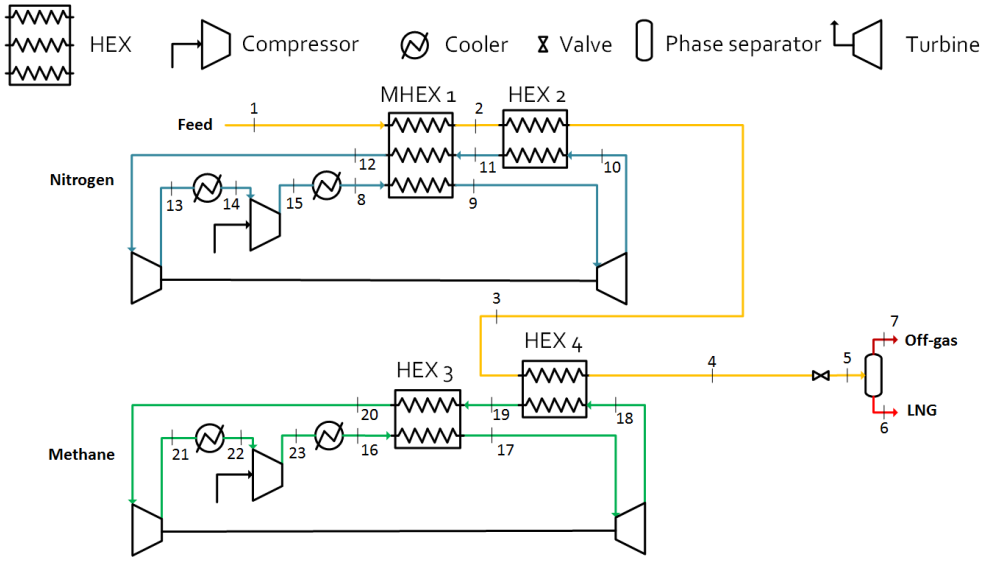

Figure 6: Dual-refrigerant configuration with methane in the bottoming cycle

3. Methods

The methods applied in this work can be presented into three steps, which reflect the three main focus areas: process modelling and evaluation, thermodynamic optimisation and economic analysis.

3.1. Process modelling and evaluation

The development of process models for the investigated expander-based configurations represents the basis for all the subsequent steps and analyses, i.e. thermodynamic optimisation and economic evaluation. The models are developed with the simulation software Aspen Plus version 7.2 [14] with the following assumptions. The natural gas feed (1 kg/s) enters the liquefaction process at 20°C and at 33 bar and is cooled in isobaric conditions down to -150°C. It is subsequently flashed to 1.7 bar for storage, resulting in a liquefaction rate of 96.4 %. Off-gases from the flash expansion are not considered in the analysis. Natural gas molar composition is reported in Table 1 and represents the typical Danish grid natural gas composition after removal of the heavy hydrocarbons and carbon dioxide.

Table 1: Natural gas feed molar composition as suggested by Kosan Crisplant A/S

CH_4	C_2H_6	C_3H_8	n-C_4H_{10}	i-C_4H_{10}	n-C_5H_{12}	i-C_5H_{12}	N_2
0.903	0.060	0.024	0.006	0.004	0.000	0.000	0.003

Refrigerant streams are set to exit the coolers at 20°C. Water is used as cooling medium and is assumed to be available at 10°C and to be heated to 40°C[1]. Thermo-physical properties are computed using the cubic equation of state of Peng and Robinson, which is widely used in the simulation of processes with hydrocarbons [15]. Pressure drops in all heat exchangers are neglected, as well as heat losses and gains. The streams exiting each heat exchanger are at the same temperature as the ones present on the same side. The polytropic efficiency of compressors is set to 82%, while the isentropic efficiency of the expanders is set to 85% [16], [17]. No mechanical losses are considered.
Based on the first law of thermodynamics, the energy balance for a liquefaction process can be written as:

$$\dot{m}_{NG}\left(h_G - h_L\right) = \dot{Q}_0 - \left(\dot{W}_{comp} - \dot{W}_{\exp}\right), \qquad (1)$$

where $\dot{m}_{NG}$ and h are the natural gas mass flow rate and specific enthalpy, respectively. $\dot{Q}_0$ is the heat rate which is rejected to the ambient, while $\dot{W}_{comp} - \dot{W}_{\exp}$ is the net power input to the cycle, i.e. the compressor power minus the expander recoverable power.
From the second law of thermodynamics, the entropy balance of a liquefaction system can be written as following:

$$\dot{m}_{NG}\left(s_G - s_L\right) + \dot{S}_{gen} = \frac{\dot{Q}_0}{T_0}, \qquad (2)$$

where s is the specific entropy of the natural gas stream and T_0 is the ambient temperature at which $\dot{Q}_0$ is rejected, expressed in Kelvin. $\dot{S}_{gen}$ is the entropy generation rate, which is zero in a reversible system, positive otherwise.

[1] These assumptions allow for the calculation of the cooler UA-value. The only exception is the propane condenser (Figure 3), for which cooling water has to exit at 20°C to achieve a 3-K temperature approach.

The combination of Equations (1) and (2) gives the exergy balance for the liquefaction system:

$$\dot{W}_{comp} - \dot{W}_{\exp} = \dot{m}_{NG}\left[\left(h_L - h_G\right) - T_0\left(s_L - s_G\right)\right] + T_0\,\dot{S}_{gen} \qquad (3)$$

When considering exergy, a remark has to be made regarding the coolers and more generally all the heat exchange blocks with only one stream. The purpose of these components is to reject heat to the ambient. For the sake of the exergy analysis this rejection is regarded as a pure exergy loss, which in rigorous terms comprises (i) the exergy destruction due to the temperature difference between the heat exchange fluids at the cooler, and (ii) the actual exergy lost to the ambient.
The minimum work required to perform the liquefaction process is obtained from the Equations (3) when imposing a zero entropy generation rate:

$$\dot{W}_{\min} = \dot{m}_{NG}\left[\left(h_L - h_G\right) - T_0\left(s_L - s_G\right)\right] \qquad (4)$$

The following performance indicators can therefore be defined for natural gas liquefaction systems:

- the specific or unit power consumption w, that is the amount of power consumed per unit of produced liquefied gas:

$$w = \frac{\dot{W}_{comp} - \dot{W}_{\exp}}{\dot{m}_{LNG}} \qquad (5)$$

- the Coefficient of Performance (COP) of the liquefaction cycle, being the ratio of the refrigeration effect (natural gas cooling load) to the net power input:

$$COP = \frac{\left|\dot{Q}_C\right|}{\dot{W}_{comp} - \dot{W}_{\exp}} = \frac{\dot{m}_{NG}\left(h_G - h_L\right)}{\dot{W}_{comp} - \dot{W}_{\exp}} \qquad (6)$$

- the exergetic efficiency, also known as Figure of Merit (FOM) of the liquefaction process in the scientific literature, which quantifies the ratio of the minimum work requirement to the actual work consumed in the process:

$$\varepsilon = \frac{\dot{W}_{\min}}{\dot{W}} = \frac{\dot{m}_{NG}\left[\left(h_L - h_G\right) - T_0\left(s_L - s_G\right)\right]}{\dot{W}_{comp} - \dot{W}_{\exp}} \qquad (7)$$

The principles of the exergy analysis are applied in order to calculate the rational efficiency defects of each individual component, δ_i defined by Kotas [18] as:

$$\delta_i = \frac{T_0\,\dot{S}_{gen,i}}{\dot{W}_{comp} - \dot{W}_{\exp}} \qquad (8)$$

The aim of the exergy analysis is to quantify how the different components contribute to the total thermodynamic irreversibilities of the cycles. For this analysis and for the calculation of the cycle exergetic efficiency the reference ambient temperature T_0 is 10°C, corresponding to the temperature of the available cooling water.

3.2. Thermodynamic optimisation

The thermodynamic optimisation is performed using a genetic algorithm developed at the École Polytechnique Fédérale de Lausanne (EPFL) by Molyneaux [19]. Two optimisation problems are addressed. First, a single-objective optimisation with the aim of minimising the net power consumption of the cycle (i.e. maximising its exergetic efficiency) is performed. It is complemented by multi-objective optimisations, with the aim of simultaneously minimising the net power consumption and the total heat transfer conductance (UA), as an indicator of the required heat transfer

area. The use of the UA-value to evaluate the system size is relevant only for systems where the overall heat transfer coefficient (U) is similar. For example, the refrigerant in expander-based systems is in gaseous state in all heat exchangers, resulting in relatively low U-values (from 80 to 750 W/m^{2}K, Table 2) compared to mixed-refrigerant systems, where phase change takes place.
The decision variables for the optimisation problem are, in general terms, the pressure levels, temperatures and flow rates of the refrigerants. The lower and upper bounds for each decision variable are set based on the available literature and on the process modelling phase, and are listed in Appendix A for the six expander-based configurations under investigation.
The optimisation problem is also subject to some practical constraints:

- the minimum temperature difference ΔT allowable in every heat exchanger is 3°C;
- the refrigerant vapour fraction at the inlet and outlet of both compressors and turbines cannot be lower than 1, to avoid liquid formation in the turbomachinery.

These constraints are highly non-linear and are handled by transforming the problem into an unconstrained one but subject to penalty functions.

3.3. Economic analysis

A simplified discounted cash flow model is applied to evaluate the economy of expander-based LNG production configurations.
The Total Capital Investment (TCI) for the liquefaction facility is determined using the Module Costing Technique, applying the cost correlations proposed by Turton et al. [20].

The purchased cost of equipment evaluated at some base conditions, C_P^0 is described by the following expression as a function of the capacity parameter *A*:

$$\log_{10} C_P^0 = k_1 + k_2 \log_{10} A + k_3 (\log_{10} A)^2 \quad (9)$$

This base cost is then adjusted for the actual working conditions of the equipment and for all the associated direct and indirect expenses with the Bare Module Cost Factor, F_{BM} :

$$C_{BM} = C_P^0 \cdot F_{BM} \quad (10)$$

The Bare Module Equipment Cost is actualised through the ratio of the CEPCI index for 2014 (576.1) to the CEPCI index for 1998 (382) and is increased of a factor 18 % to account for contingencies and fees [21]. The Total Capital Investment is then computed as:

$$TCI = 1.18 \sum_{i=1}^{n} C_{BM,i} \quad (11)$$

This methodology is applied for centrifugal compressors, compressor drives, expanders, phase separators and refrigerant coolers.
Heat exchanger capital costs are provided by the flat-plate heat exchanger manufacturer SWEP. The heat transfer area is based on the value of heat duty given by Aspen Plus and calculated applying the U-values reported in Table 2 for the different types of heat exchange, estimated using SWEP software [22].

Table 2: U-values in W/m^{2}K for the different heat exchange possibilities in the analysed expander-based processes [22]

Cold-side fluid	Hot-side fluid				
	Nitrogen	Methane	Gaseous hydrocarbon	Condensing hydrocarbon	Liquid hydrocarbon
Nitrogen – medium pressure	250	-	225	400	550
Methane – medium pressure	-	375	375	750	750
Methane – low pressure	-	80	80	100	150

Operation and maintenance costs are determined based on the following inputs:

- plant maintenance cost is set to be 2 % of the total capital investment;
- natural gas feed price is set equal to 14.85 €/MWh (HHV basis) as suggested by Kosan Crisplant A/S;
- electricity price is 8.79 c€/kWh as in the third EU Quarterly Report on 2015 European Electricity Markets for Danish industrial consumers [23]. Electricity consumption is given by the total compressor power requirement, thus expander power production is disregarded;
- LNG price is assumed to be 28 €/MWh (HHV basis) as suggested by Kosan Crisplant A/S;
- unitary cost for nitrogen is 3.5 $/kg, while the unitary cost for methane and propane is 103.6 $/kg. The total refrigerant charge is calculated assuming a specific charge of 1.6 kg per kW of cooling effect [24] and a Bare Module Factor of 1.25 [21].

The economic performance indicator is the Unitary Profit (UP), defined as the profit per mass unit of produced LNG. It is calculated on a yearly basis as the ratio of the annual profit to the yearly LNG production. The initial investment is annualised using the so-called PMT factor defined as following:

$$PMT = \frac{i}{1-(1+i)^{-LT}} \tag{12}$$

The discount rate i is 8 %, while a lifetime (LT) of 40 years is assumed for LNG production plants according to the Danish Maritime Authority [25].
The economic evaluation of the six expander-based configurations is performed based on the operating conditions that yield the minimum power consumption.

4. Results

Table 3 reports the main thermodynamic performance indicators for the optimised expander-based processes together with the net power consumption and the total UA-value for the cycle, which gives an indication of the required heat transfer area. The optimal values for the decision variables of the optimisation problems are listed in Tables from B.1 to B.6 in Appendix B.
The most effective design is the dual-refrigerant process. Additionally it is more beneficial to use nitrogen for the liquefaction and sub-cooling of natural gas, as this choice enables a greater reduction in net power consumption with a lower requirement in terms of heat transfer area.

Table 3: Summary of the Single-Objective Optimisation results for the developed models

	$\dot{W}_{net}$ [kW]	Total UA-value [kW/K]	COP [-]	w [kJ/kg $_{LNG}$]	FOM [%]
Single-expander	2475	137.4	0.320	2568	15.50
Single-expander with two-stage comp.	1796	133.8	0.441	1863	21.36
Propane pre-cooled single-expander	1559	176.2	0.509	1617	24.60
Dual-expander	1431	280.0	0.554	1484	26.81
Dual-refrigerant with N_2 sub-cooling	1288	285.9	0.616	1336	29.79
Dual-refrigerant with CH_4 sub-cooling	1429	342.2	0.555	1482	26.85

Figures 7 to 10 depict the Composite Curves and the temperature profiles (Figure 9 (b) and Figure 10 (b)) at the cryogenic heat exchangers for the six optimised configurations.
The increase in thermodynamic efficiency is strictly correlated to two main design choices.
On the one hand, an inter-cooled two-stage compression process allows bringing the adiabatic compression closer to an isothermal one, leading to a thermodynamic superiority over the single-expander process. Moreover, it enables having a greater total pressure ratio, which leads to a reduction of the required refrigerant mass flow rate and a closer match of the temperature profiles (Figure 7 (b)).

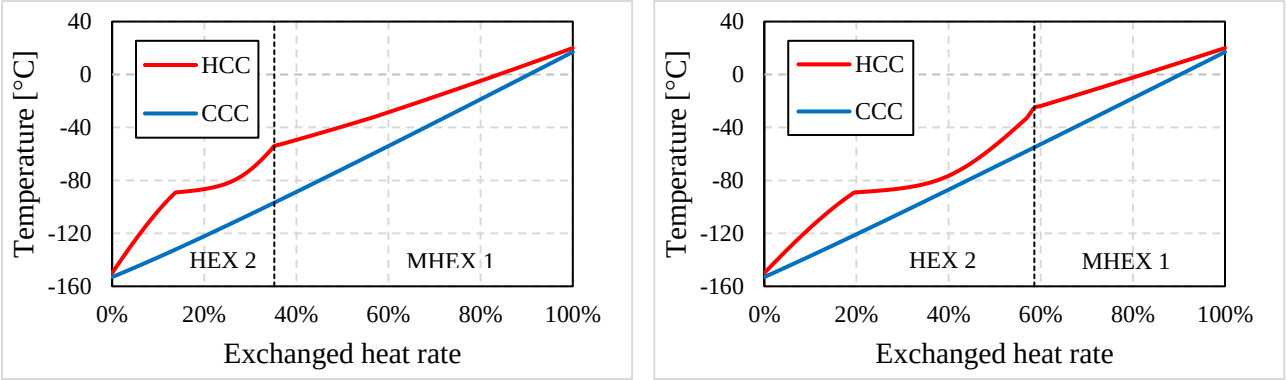

Figure 7: Composite Curves for the optimised single-expander configuration with one (a) and two (b) compression stages

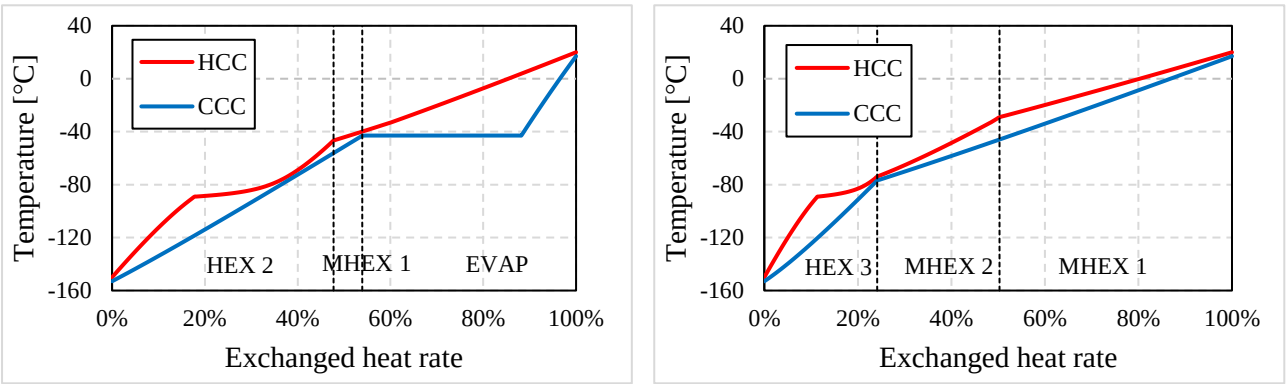

Figure 8: Composite Curves for the optimised propane pre-cooled single-expander configuration (a) and for the dual-expander configuration (b)

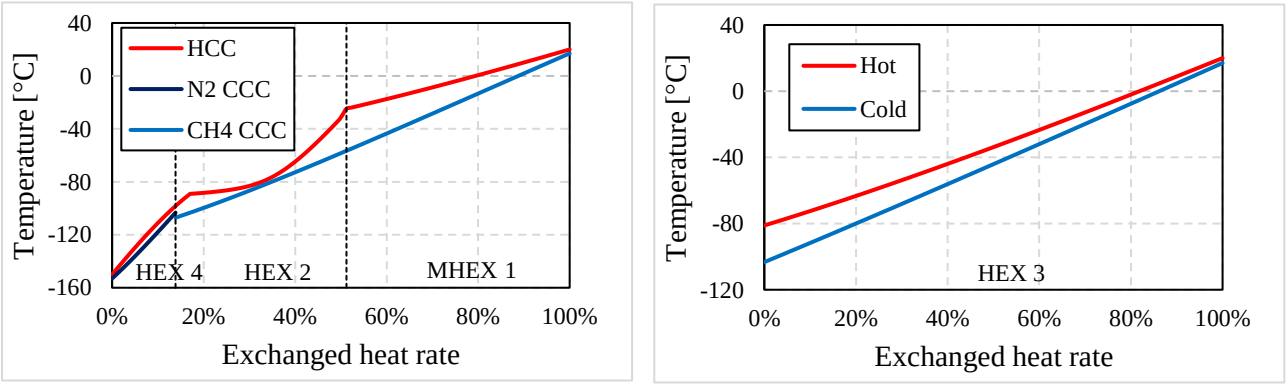

Figure 9: Composite Curves (a) and temperature profile (b) for the optimised dual-refrigerant configuration having nitrogen in the bottoming refrigeration cycle

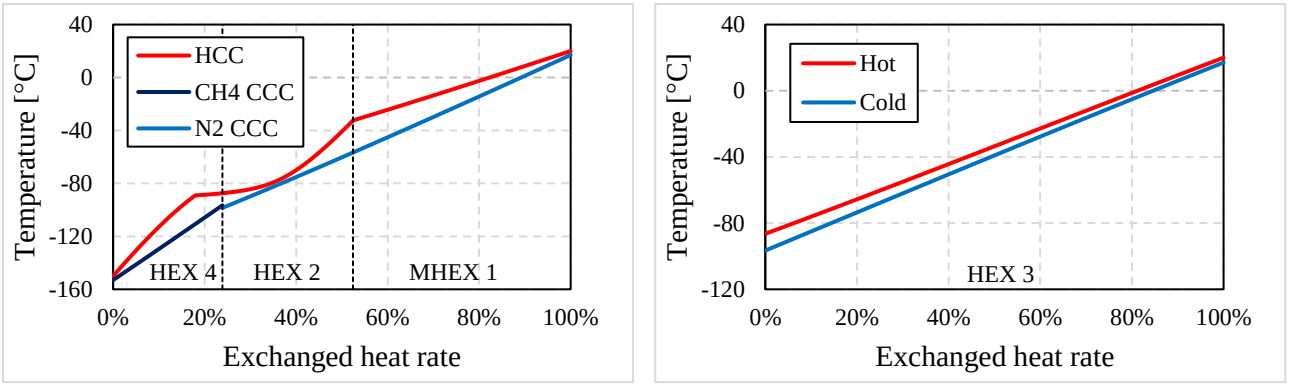

Figure 10: Composite Curves (a) and temperature profile (b) for the optimised dual-refrigerant configuration having methane in the bottoming refrigeration cycle

On the other hand, the five developments of the single-expander configuration lead to a reduction of the mean temperature difference at the cryogenic heat exchangers, thus to a reduction of the net power consumption of the liquefaction process. The area between the Composite Curves is related to the exergy destruction in the heat exchange process. This can be graphically noticed in Figure 11, which gives an overview of the exergy destructions and losses in the six optimised expander-based processes.

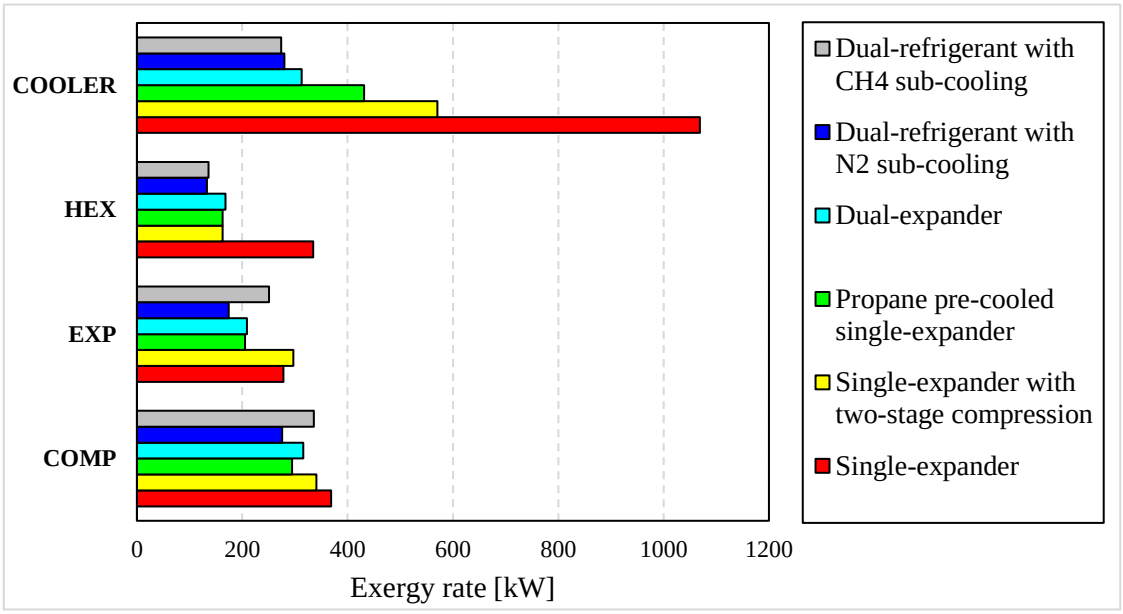

Figure 11: Exergy destructions and losses grouped for component category for the optimised expander-based configurations

The cooler is responsible for the greatest share of exergy destruction within the liquefaction system, because of (i) the gap between the temperature profiles of the refrigerant and cooling water, and (ii) the large losses of energy dissipated to the environment. This trend is particularly marked in the least efficient configurations. It is then followed by the compression, expansion and cryogenic refrigeration processes.

However, the exergy destruction taking place in the cooler actually results from a low performance of the compression process, since higher temperatures are reached at the compressor outlet and larger quantities of heat are discharged.

All in all, the greatest exergy destruction occurs in the compressor, followed by the expander. These processes can only be improved by using more efficient components or by compressing/expanding in multiple stages. Finally, the exergy destruction in the cryogenic heat exchanger is caused by the irreversibilities of the heat transfer process. It can be reduced only by allowing closer temperature matches, which is possible at the expense of larger heat exchangers.
The results from the Multi-Objective Optimisations are collected and illustrated by the Pareto fronts in Figure 12. The efficiency improvement of the expander-based configurations is achieved at the expense of a higher total UA-value, which ranges between 50 kW/K and 275 kW/K.
The low-pressure level is generally the decision variable showing the greatest correlation with the two conflicting objectives. More specifically, a higher low-pressure level has to be sought if the aim is to minimise the net power consumption. This, however, shrinks the available temperature difference for the natural gas sub-cooling, thus impacting on the heat transfer area.

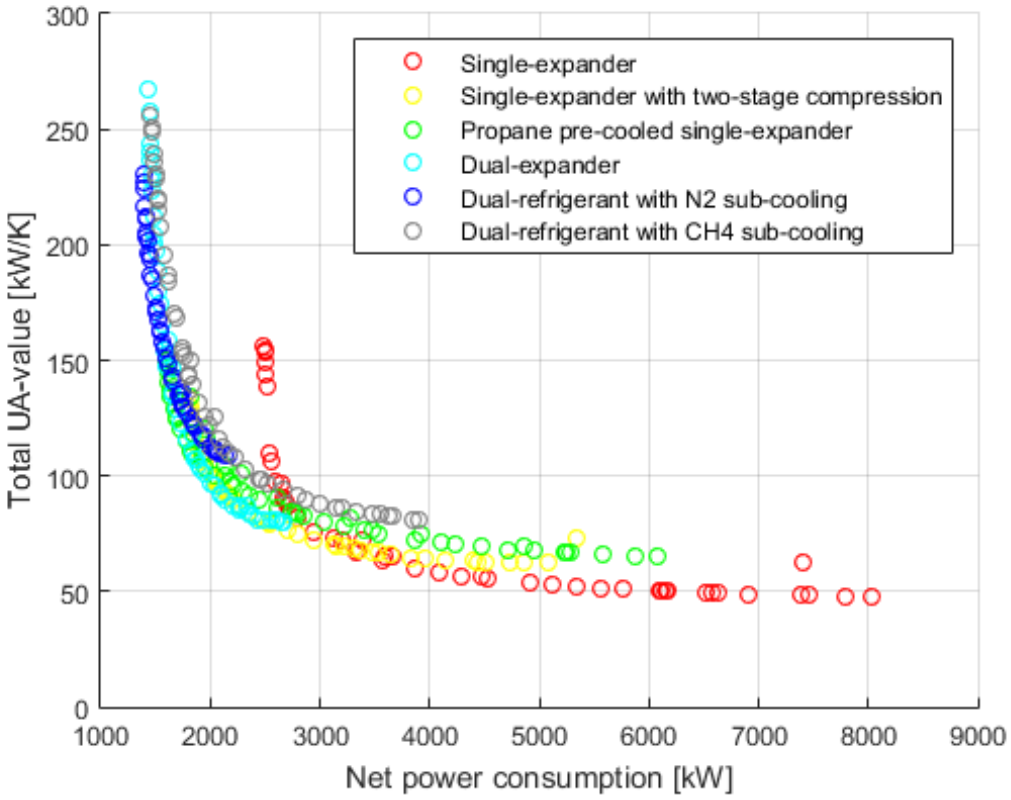

Figure 12: Pareto fronts for the six analysed expander-based configurations

The outcome of the Multi-Objective Optimisations represents the basis for analysing natural gas liquefaction cycles from an economic point of view. Table 4 reports the summary of the economic performance of the expander-based configurations.
Yearly revenues are unchanged for the different configurations, depending solely on the liquefaction rate, and amount to 91.3 MDKK per year.
The three most promising configurations are, in descending order, N_2 sub-cooling dual-refrigerant cycle, CH_4 sub-cooling dual-refrigerant cycle and propane pre-cooled single-expander cycle. The least favourable alternative is the single-expander cycle with one compression stage.
Overall it can be inferred that the configurations achieving the lowest net power consumption are the ones yielding the best economic results. Nevertheless some cases deviate from this general trend. The propane pre-cooled single-expander cycle results to be more favourable than dual-expander configurations given the fewer equipment items and the simpler cycle design.

Table 4: Total Capital Investment, O&M cost and Unitary Profit for the six expander-based configurations

Configuration	TCI [MDKK]	O&M [MDKK/year]	UP [DKK/kg $_{LNG}$]
Single-expander	141	69.9	0.330
Single-expander with two-stage comp.	121	65.9	0.528
Propane pre-cooled single-expander	98.6	63.9	0.661
Dual-expander	107	63.5	0.650
Dual-refrigerant with N_2 sub-cooling	95.7	59.3	0.828
Dual-refrigerant with CH_4 sub-cooling	126	60.7	0.693

4. Discussion

In this section the presented results are discussed and their limitations highlighted. The aim of the present work is to understand which design improvements can be adopted to enhance the efficiency of the expander-based configurations, which are penalized from this point of view with respect to other liquefaction concepts. Thermodynamic optimisation is needed in order to quantify the influence of the design choices in terms of net power consumption and required heat transfer area.

The need for a rigorous optimisation procedure through a genetic algorithm is justified by the relatively high number of decision variables that expander-based cycles present, usually pressure, temperature levels and refrigerant flow rates.

Further reductions in power consumption could have been achieved by coupling two design improvement steps, i.e. dual expansion with a pre-cooling cycle or pre-cooling single-expander cycle with inter-cooled two-stage compression. As an example, He et al. [12] investigate and optimise a dual-turbine cycle with different pressure ratio adding R410A pre-cooling and inter-cooled three-stage compression, achieving a Figure of Merit of 56 %. This is not covered in the present work and could represent a future development. However, this goes in the direction of a more complex cycle design, which is usually avoided for small-scale liquefaction plants.

It could also be argued that the dual-refrigerant alternatives perform the best as they combine the dual-refrigerant concept with the inter-cooled two-stage compression process. This modelling choice is adopted as these cycles are designed in such a way in "real-life" applications. Moreover the inter-cooled two-stage compression is also implemented in the considered dual-expander configuration, therefore the provided ranking is considered robust.

Comparing the obtained results with the ones presented in the literature some differences can be highlighted.

For instance He et al. [12] claim that R410A is the most effective pre-cooling refrigerant, whereas in this work only propane is considered, based on the outcome presented in [26]. This difference originates from the variation range which is set for the pre-cooling temperature, as the authors set a lower bound of -44°C for R410A and of -37°C for propane. On one hand this penalises the propane alternative, on the other hand it avoids having sub-atmospheric refrigerant in the pre-cooling cycle, a condition which is not required and fulfilled in the present work.

As to dual-expander cycles, Khan et al. [27] achieve a unit energy consumption of 2700 kJ/kg for the base-case single-expander cycle and of 1800 kJ/kg for the dual-turbine cycle (relative difference of -33 %). Values are slightly higher than the ones achieved in this work, mainly because authors select lower isentropic efficiency for the turbo-machinery (0.75 for both compressors and expanders) and a lower natural gas outlet temperature (-158.5°C). However, this difference is mitigated by the presence of an inter-cooled four-stage compression process.

On the contrary Chang et al. [28] show that the dual-expander alternative achieves an exergy efficiency higher by 15%-points compared to the single-expander cycle. This figure is slightly higher than in the present work and can be imputed to the differences in the composition of the natural gas feed.

Very little is found in the literature about economic analyses of liquefaction processes – one of the main reasons is that three-flow heat exchangers are complex components designed only by few specific companies. Most of those economic data are confidential, as pinpointed in the case of the PRICO cycle by Morosuk et al.[29]. In most cases, this aspect is addressed by investigating the trade-off between power consumption and heat transfer area, which partly reflects the trade-off between investment and operation cost, as the capital expenditure may be dominated by the turbo-machinery cost.

Economic figures are determined combining thermodynamic results with cost functions, which reliability is therefore crucial to obtain sensible results. The correlations given by Turton et al. [20] are widely applied for preliminary cost estimation of chemical plants, with an uncertainty of +/- 30%. Nevertheless, they may be unsuitable given the peculiarities of a cryogenic application like natural gas liquefaction, especially since little is known on the costs of multiple-stream plate-fin heat exchangers.

Additionally, in the present study the following simplifications are adopted in the discounted cash flow analysis. No tax and financial considerations are included. The choice of an 8 %-discount rate may be argued as well, since the industry-related risk for a small-scale LNG facility can contribute to a considerable increase in the cost of capital. In light of these simplifications the aim of this analysis is not to give a realistic indication about the economic profitability of a LNG production facility in the Danish context, but rather to couple thermodynamic results with economic data to further understand the interplay between them.

As aforementioned, performing the economic comparison on thermodynamic optimum cycles is a key assumption. This might be unfair as the economic optimum is likely not to coincide with the thermodynamic one. To understand that, a series of Multi-Objective Optimisations is performed on the least and the most economically favourable alternatives with the aim of simultaneously minimising compressor and heat exchange network investment costs. Results are displayed in Figure 13 on the left for the single-expander cycle with one compression stage and in Figure 13 on the right for the N_2 sub-cooling dual-refrigerant cycle.

As expected compressor investment cost increases together with power consumption, while the investment cost relative to the heat exchange network decreases. However it can be seen that compressor cost is much higher than the investment in heat exchangers for all cases.

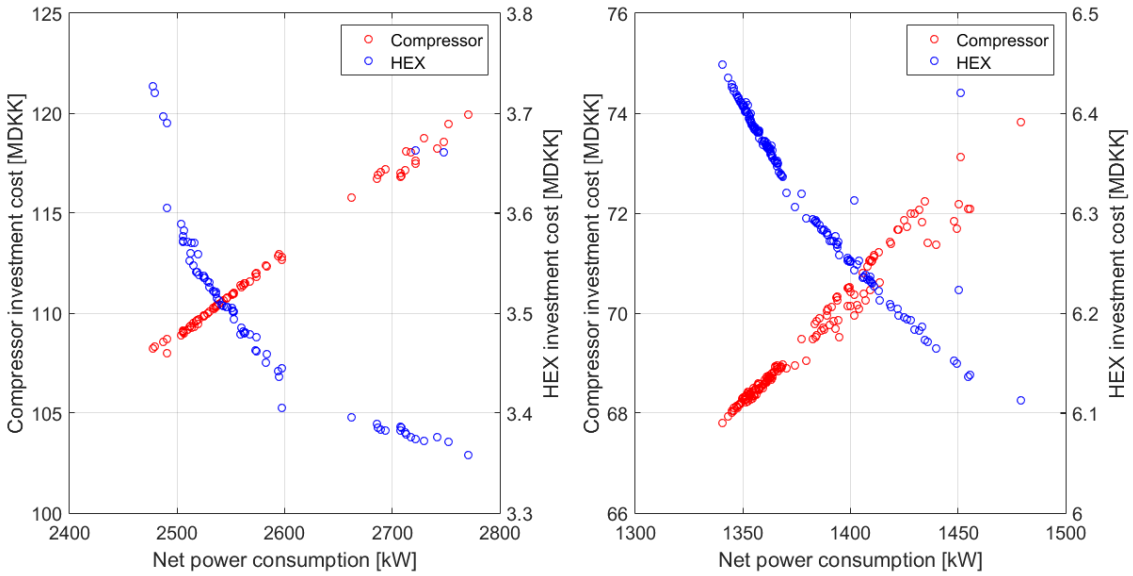

Figure 13: Pareto fronts for the investment cost Multi-Objective Optimisations on the single-expander cycle (left) and on the dual-refrigerant cycle with N_2 sub-cooling (right). HEX investment cost is reported on the secondary vertical axis

Given the same increase in net power consumption, the increase in investment associated to the compressors is one order of magnitude greater than the decrease in investment relative to heat exchangers. As a consequence, no trade-off between compressor and heat exchanger cost occurs, therefore the thermodynamic optimum coincides with the economic one.
This observation sets the basis for future developments in terms of cost data validation and, if applicable, research of the economic optimum for the different expander-based configurations.

5. Conclusion

This paper focuses on the thermodynamic and economic analysis of different LNG production configurations. Interest in LNG is growing in among others the shipping sector due to economic advantages over oil alternatives and stricter environmental regulations for shipboard NO_x and SO_x emissions.
LNG production is highly energy intensive, therefore a thorough thermodynamic analysis and optimisation is required to reduce the compression power consumption. Focus is put on expander-based configurations and six models are developed using the software Aspen Plus. The modelling stage highlights two main drivers for efficiency improvements: the compression process design and the reduction of the mean temperature difference at the cold box.
Inter-cooled multi-stage compression should be preferred to the single-stage one.
Secondly, the temperature difference at the cold box is a decisive factor for the exergy destruction during the liquefaction process and can be reduced by:

- adding a pre-cooling stage;
- introducing a dual-expander process;
- implementing a dual-refrigerant cycle.

Thermodynamic optimisation by means of genetic algorithm is performed to quantify the efficiency improvements. The base case is the single-expander cycle with one compression stage, which achieves a net power consumption of 2475 kW and an exergetic efficiency of 15.5 %.
Adopting an inter-cooled two-stage compression reduces the power consumption by 27 %. Pre-cooling of natural gas is beneficial and leads to a 37 %-saving in net power consumption. Adopting a dual expansion process reduces net power consumption by 42 %.
The highest benefit is recorded when choosing a dual-refrigerant cycle in which both refrigerants are used in closed loops. Nitrogen is found to be more suitable than methane for natural gas cooling at lower temperature range. Net power consumption is reduced by 48 % with respect to the base case. Correspondingly, the exergetic efficiency of the liquefaction cycle is 30 %.
Exergy analysis is performed on the thermodynamic optimal cycles. Components' rational efficiency defects are computed to highlight the distribution of exergy destructions and losses. Exergy loss at refrigerant coolers generally represents the largest dissipation of useful work. The waste heat should be utilised given the high temperature level of the refrigerant streams at cooler inlets. Compression processes are responsible for the greatest share of exergy destruction, followed by expansions.
The reduction in power consumption comes at the expense of heat transfer area. This is pinpointed through a series of Multi-Objective Optimisations aiming at simultaneously minimising the net power consumption and the overall heat network conductance. The latter is found to range between 50 kW/K and 275 kW/K for the expander-based concept.
The existence of a trade-off between power consumption and heat transfer area justifies an economic analysis for the LNG production configurations. A simplified Discounted Cash Flow model is set up and the different alternatives are compared based on their Unitary Profit. The most profitable alternative is the dual-refrigerant configuration with N_2 sub-cooling, which achieves 0.83 DKK per kg of produced LNG.
The reliability of economic outcomes is discussed, as it mostly depends on the employed cost correlations. The ones used for this work make compressors the most capital-intensive components, leading to the coincidence of thermodynamic and economic optimum.

Acknowledgments

The authors thank Kosan Crisplant and SWEP for the given material and feedback, in particular with respect to the economic correlations used in this research. The second and third authors thank the Danish societal partnership Blue INNOship, which is partly funded by the Innovation Fund Denmark under File No. 155-2014-10 and the Danish Maritime Fund.

Appendix A

This appendix lists the decision variables considered in the optimisation problem, for the six investigated layouts.

Table A.1: Decision variables for the optimisation of the single-expander cycle

Parameter	Variable	Unit	Range
High-pressure level	P_7	bar	[60,130]
Low-pressure level	P_9	bar	[1,20]
Expander inlet temperature	T_8	°C	[-100,0]
Nitrogen flow rate	$\dot{m}_{N_2}$	kg/s	[5,20]

Table A.2: Decision variables for the optimisation of the single-expander cycle with two-stage compression

Parameter	Variable	Unit	Range
High-pressure level	P_7	bar	[60,130]
Low-pressure level	P_9	bar	[1,10]
Intermediate-pressure level	P_{13}	bar	[11,59]
Expander inlet temperature	T_8	°C	[-100,0]
Nitrogen flow rate	$\dot{m}_{N_2}$	kg/s	[5,20]

Table A.3: Decision variables for the optimisation of the propane pre-cooled single-expander cycle

Parameter	Variable	Unit	Range
Nitrogen high pressure	P_9	bar	[60,130]
Nitrogen low pressure	P_{11}	bar	[1,10]
Expander inlet temperature	T_{10}	°C	[-100,-45]
Nitrogen flow rate	$\dot{m}_{N_2}$	kg/s	[1,15]
Propane high pressure	P_{18}	bar	[8.37,42.5]
Propane low pressure	P_{16}	bar	[0.5,5]
Pre-cooling temperature	T_2	°C	[-40,0]

Table A.4: Decision variables for the optimisation of the dual-expander cycle

Parameter	Variable	Unit	Range
High-pressure level	P_8	bar	[80,130]
Low-pressure level	P_{14}	bar	[1,25]
Intermediate-pressure level	P_{10}	bar	[30,75]
HP expander inlet temperature	T_9	°C	[-45,0]
LP expander inlet temperature	T_{13}	°C	[-100,-50]
Nitrogen flow rate	$\dot{m}_{N_2}$	kg/s	[5,20]
Split fraction	$\dot{m}_{13}/\dot{m}_{10}$	-	[0.05,0.5]

Table A.5: Decision variables for the optimisation of the dual-refrigerant cycle having nitrogen in the bottoming refrigeration cycle

Parameter	Variable	Unit	Range
Nitrogen high pressure	P_{16}	bar	[60,90]
Nitrogen low pressure	P_{18}	bar	[5,30]
N_2 expander inlet temperature	T_{17}	°C	[-100,-50]
Nitrogen flow rate	$\dot{m}_{N_2}$	kg/s	[1,5]
Methane high pressure	P_8	bar	[60,90]
Methane low pressure	P_{10}	bar	[5,30]
CH_4 expander inlet temperature	T_9	°C	[-50,0]
Methane flow rate	$\dot{m}_{CH_4}$	kg/s	[1,5]
NG intermediate temperature	T_3	°C	[-120,-20]

Table A.6: Decision variables for the optimisation of the dual-refrigerant cycle having methane in the bottoming refrigeration cycle

Parameter	Variable	Unit	Range
Nitrogen high pressure	P_8	bar	[60,130]
Nitrogen low pressure	P_{10}	bar	[1,30]
N_2 expander inlet temperature	T_9	°C	[-100,0]
Nitrogen flow rate	$\dot{m}_{N_2}$	kg/s	[1,8]
Methane high pressure	P_{16}	bar	[2.5,20]
Methane low pressure	P_{18}	bar	[0.1,2]
CH_4 expander inlet temperature	T_{17}	°C	[-130,-80]
Methane flow rate	$\dot{m}_{CH_4}$	kg/s	[1,8]
NG intermediate temperature	T_3	°C	[-120,-20]

Appendix B

In this Appendix the optimal values for the decision variables are listed for the six optimised expander-based configurations.

Table B.1: Optimal values of the decision variables for the optimisation of the single-expander cycle

Parameter	Variable	Unit	Range	Optimal value
High-pressure level	P_7	bar	[60,130]	116.8
Low-pressure level	P_9	bar	[1,20]	12.6
Expander inlet temperature	T_8	°C	[-100,0]	-54.1
Nitrogen flow rate	$\dot{m}_{N_2}$	kg/s	[5,20]	8.7

Table B.2: Optimal values of the decision variables for the optimisation of the single-expander cycle with two-stage compression

Parameter	Variable	Unit	Range	Optimal value
High-pressure level	P_7	bar	[60,130]	129.6
Low-pressure level	P_9	bar	[1,10]	7.8
Intermediate-pressure level	P_{13}	bar	[11,59]	33.6
Expander inlet temperature	T_8	°C	[-100,0]	-25.2
Nitrogen flow rate	$\dot{m}_{N_2}$	kg/s	[5,20]	6.3

Table B.3: Optimal values of the decision variables for the optimisation of the propane pre-cooled single-expander cycle

Parameter	Variable	Unit	Range	Optimal value
Nitrogen high pressure	P_9	bar	[60,130]	108
Nitrogen low pressure	P_{11}	bar	[1,10]	9.9
Expander inlet temperature	T_{10}	°C	[-100,-45]	-46.6
Nitrogen flow rate	$\dot{m}_{N_2}$	kg/s	[1,15]	5.6
Propane high pressure	P_{18}	bar	[8.37,42.5]	8.37
Propane low pressure	P_{16}	bar	[0.5,5]	0.98
Pre-cooling temperature	T_2	°C	[-40,0]	-39.9

Table B.4: Optimal values of the decision variables for the optimisation of the dual-expander cycle

Parameter	Variable	Unit	Range	Optimal value
High-pressure level	P_8	bar	[80,130]	116.5
Low-pressure level	P_{14}	bar	[1,25]	18.5
Intermediate-pressure level	P_{10}	bar	[30,75]	50.8
HP expander inlet temperature	T_9	°C	[-45,0]	-29
LP expander inlet temperature	T_{13}	°C	[-100,-50]	-73.9
Nitrogen flow rate	$\dot{m}_{N_2}$	kg/s	[5,20]	13.8
Split fraction	$\dot{m}_{13}/\dot{m}_{10}$	-	[0.05,0.5]	0.36

Table B.5: Optimal values of the decision variables for the optimisation of the dual-refrigerant cycle having nitrogen in the bottoming refrigeration cycle

Parameter	Variable	Unit	Range	Optimal value
Nitrogen high pressure	P_{16}	bar	[60,90]	74.8
Nitrogen low pressure	P_{18}	bar	[5,30]	13.8
N_2 expander inlet temperature	T_{17}	°C	[-100,-50]	-81.1
Nitrogen flow rate	$\dot{m}_{N_2}$	kg/s	[1,5]	3.0
Methane high pressure	P_8	bar	[60,90]	85.8
Methane low pressure	P_{10}	bar	[5,30]	19.1
CH_4 expander inlet temperature	T_9	°C	[-50,0]	-24.8
Methane flow rate	$\dot{m}_{CH_4}$	kg/s	[1,5]	3.8
NG intermediate temperature	T_3	°C	[-120,-20]	-98.3

Table B.6: Optimal values of the decision variables for the optimisation of the dual-refrigerant cycle having methane in the bottoming refrigeration cycle

Parameter	Variable	Unit	Range	Optimal value
Nitrogen high pressure	P_8	bar	[60,130]	77.4
Nitrogen low pressure	P_{10}	bar	[1,30]	22.7
N_2 expander inlet temperature	T_9	°C	[-100,0]	-32.4
Nitrogen flow rate	$\dot{m}_{N_2}$	kg/s	[1,8]	7.4
Methane high pressure	P_{16}	bar	[2.5,20]	13.2
Methane low pressure	P_{18}	bar	[0.1,2]	1.9
CH_4 expander inlet temperature	T_{17}	°C	[-130,-80]	-86.4
Methane flow rate	$\dot{m}_{CH_4}$	kg/s	[1,8]	2.5
NG intermediate temperature	T_3	°C	[-120,-20]	-87.4

Nomenclature

Abbreviations

COP Coefficient of Performance, -

FOM Figure of Merit, -

LNG Liquefied Natural Gas

NG Natural Gas

UP Unitary Profit, DKK/kg $_{LNG}$

TCI Total Capital Investment, MDKK

Greek symbol

ε exergetic efficiency, -

δ rational efficiency defect, -

Δ difference

Roman symbols

A capacity parameter for cost correlations

C_{BM} Bare Module Equipment Cost, DKK

C_p^0 base-condition purchased cost of equipment, DKK

F_{BM}	Bare Module Cost Factor, -
h	specific enthalpy, kJ/kg
i	discount rate, -
LT	lifetime, years
$\dot{m}$	mass flow rate, kg/s
P	pressure, bar
$\dot{Q}$	heat flow, kW
s	specific entropy, kJ/kgK
$\dot{S}_{gen}$	entropy generation rate, kW/K
T	temperature, °C
U	heat exchanger overall heat transfer coefficient, kW/m^{2}K
UA	heat exchanger UA-value, kW/K
w	unit energy consumption, kJ/kg
$\dot{W}$	mechanical power, kW

Subscripts and superscripts

comp	compressor
exp	expander
G	gas
i	component index
L	liquid
min	minimum
0	ambient

References

[1] "Liquefied Natural Gas: Understanding the Basic Facts," United States of America, 2005.

[2] U. Nations, "International Marine Organization." [Online]. Available: http://www.imo.org/en/About/Pages/Default.aspx. [Accessed: 01-Feb-2016].

[3] E. P.-M. of E. and F. of D. Agency, "Reducing shipping emissions." [Online]. Available: http://eng.mst.dk/topics/air/reducing-shipping-emissions/. [Accessed: 01-Dec-2015].

[4] I. G. Union, "World LNG report," 2015.

[5] C. Philips, "Technical Brochure." .

[6] B. Austbø, S. W. Løvseth, and T. Gundersen, "Annotated bibliography-Use of optimization in LNG process design and operation," *Comput. Chem. Eng.*, vol. 71, pp. 391–414, 2014.

[7] A. Finn, "Technology choices," *Hydrocarb. Eng.*, vol. 11, no. SUPPL., pp. 55–58, 2006.

[8] W. S. Cao, X. S. Lu, W. S. Lin, and A. Z. Gu, "Parameter comparison of two small-scale natural gas liquefaction processes in skid-mounted packages," *Appl. Therm. Eng.*, vol. 26, no. 8–9, pp. 898–904, 2006.

[9] C. W. Remeljej and A. F. A. Hoadley, "An exergy analysis of small-scale liquefied natural gas (LNG) liquefaction processes," *Energy*, vol. 31, no. 12, pp. 1669–1683, 2006.

[10] G. Shah, Nipen M and Hoadley, Andrew FA and Rangaiah, "Inherent safety analysis of a propane precooled gas-phase liquefied natural gas process," *Ind. Eng. Chem. Res.*, vol. 48, no. 10, pp. 4917--4927, 2009.

[11] L. Castillo and C. A. Dorao, “Influence of the plot area in an economical analysis for selecting small scale LNG technologies for remote gas production,” *J. Nat. Gas Sci. Eng.*, vol. 2, no. 6, pp. 302–309, 2010.
[12] T. B. He and Y. L. Ju, “Performance improvement of nitrogen expansion liquefaction process for small-scale LNG plant,” *Cryogenics (Guildf).*, vol. 61, pp. 111–119, 2014.
[13] H. M. Chang, “A thermodynamic review of cryogenic refrigeration cycles for liquefaction of natural gas,” *Cryogenics (Guildf).*, vol. 72, pp. 127–147, 2015.
[14] A. Technology, “Aspen Plus.” [Online]. Available: http://www.aspentech.com/products/engineering/aspen-plus/.
[15] F. Dauber and R. Span, “Modelling liquefied-natural-gas processes using highly accurate property models,” *Appl. Energy*, vol. 97, pp. 822–827, 2012.
[16] W. Ransbarger, “A fresh look at LNG process efficiency,” *Hydrocarb. Eng.*, vol. 12, no. SUPPL., 2007.
[17] A. J. Finn, “Are floating LNG facilities viable options?,” *Hydrocarb. Process.*, vol. 88, no. 7, pp. 31–39, 2009.
[18] T. J. Kotas, *The Exergy Method of Thermal Plant Analysis*. Malabar, USA: Krieger Publishing, 1995.
[19] I. E. S. Laboratory (LENI), “OSMOSE Platform.” [Online]. Available: http://leni.epfl.ch/osmose. [Accessed: 01-Jun-2016].
[20] R. Turton, R. C. Bailie, W. B. Whiting, J. A. Shaeiwitz, and D. Bhattacharyya, *Analysis, Synthesis and Design of Chemical Processes*, Fourth. Prentice Hall, 2012.
[21] A. Toffolo, A. Lazzaretto, G. Manente, and M. Paci, “A multi-criteria approach for the optimal selection of working fluid and design parameters in Organic Rankine Cycle systems,” *Appl. Energy*, vol. 121, pp. 219–232, 2014.
[22] SWEP, “SSP Calculation Software.” [Online]. Available: http://www.swep.net/support/ssp-calculation-software/. [Accessed: 01-May-2016].
[23] E. Commission, “Quarterly Report on European Electricity Markets,” 2015.
[24] F. Poggi, H. Macchi-Tejeda, D. Leducq, and A. Bontemps, “Refrigerant charge in refrigerating systems and strategies of charge reduction,” *Int. J. Refrig.*, vol. 31, no. 3, pp. 353–370, 2008.
[25] D. M. Authority, “North European LNG Infrastructure Project.”
[26] M. Nagy, “Techno-economic analysis of LNG production alternatives,” Technical University of Denmark - DTU, 2016. [Online]. Available on DTU Library website
[27] M. S. Khan, S. Lee, M. Getu, and M. Lee, “Knowledge inspired investigation of selected parameters on energy consumption in nitrogen single and dual expander processes of natural gas liquefaction,” *J. Nat. Gas Sci. Eng.*, vol. 23, no. January 2004, pp. 324–337, 2015.
[28] H. M. Chang, J. H. Park, K. S. Cha, S. Lee, and K. H. Choe, “Modified Reverse-Brayton Cycles for Efficient Liquefaction of Natural Gas,” pp. 435–442, 2012.
[29] T. Morosuk, S. Tesch, A. Hiemann, G. Tsatsaronis, and N. Bin Omar, “Evaluation of the PRICO liquefaction process using exergy-based methods,” *J. Nat. Gas Sci. Eng.*, vol. 27, pp. 23–31, 2015.